The Rate of Lipid Transfer during Fusion Depends on the Structure of Fluorescent Lipid Probes: A New Chain-Labeled Lipid Transfer Probe Pair†

Vladimir S. Malinin,‡,§ Md. Emdadul Haque,§ and Barry R. Lentz*

Department of Biochemistry and Program in Molecular/Cell Biophysics, University of North Carolina, Chapel Hill, North Carolina 27599-7260

Received March 21, 2001; Revised Manuscript Received May 14, 2001

ABSTRACT: A number of fluorescent probes have been used to follow membrane fusion events, particularly intermixing of lipids. None of them is ideal. The most popular pair of probes is NBD-PE and Rh-PE, in which the fluorescent groups are attached to the lipid headgroups, making them sensitive to changes in the surrounding medium. Here we present a new assay for monitoring lipid transfer during membrane fusion using the acyl chain tagged fluorescent probes BODIPY500-PC and BODIPY530-PE. Like the NBD-PE/Rh-PE assay, this assay is based on fluorescence resonance energy transfer (FRET) between the donor, BODIPY500, and the acceptor, BODIPY530. The magnitude of FRET is sensitive to the probe surface concentration, allowing one to detect movement of probes from labeled to unlabeled vesicles during fusion. The high quantum yield of fluorescence, high efficiency of FRET (R_o is estimated to be ~60 Å), photostability, and localization in the central hydrophobic region of a bilayer all make this pair of probes quite promising for detecting fusion. We have compared this and two other lipid mixing assays for their abilities to detect the initial events of poly(ethylene glycol) (PEG)-mediated fusion of small unilamellar vesicles (SUVs). We found that the BODIPY500/530 assay showed lipid transfer rates consistent with those obtained using the DPHpPC self-quenching assay, while lipid mixing rates measured with the NBD-PE/Rh-PE RET assay were significantly slower. We speculate that the bulky labeled headgroups of NBD-PE and especially Rh-PE molecules hamper movement of probes through the stalk between fusing vesicles, and thus reduce the apparent rate of lipid mixing.

Monitoring intermixing or dilution of fluorescent lipids between labeled and unlabeled vesicles has been an important tool for revealing the molecular mechanism of membrane fusion. It is believed that lipid mixing marks recognizable steps in the fusion process: merging of the outer leaflets at stalk formation and, to some extent, merging of the inner leaflets accompanying fusion pore formation. Three types of assays have been reported in the literature for membrane lipid mixing based on changes of fluorescent probe signals, such as excimer formation (*1*, *2*), fluorescence self-quenching (*3*−*5*), and fluorescence resonance energy transfer (FRET)[1] (*6*, *7*). Among them, one can list an assay using fluorescence energy transfer between N-NBD-PE and N-Rh-PE and an assay using excited-state complex formation of DPH-PC. FRET-based assays are currently the most popular assays for monitoring lipid mixing. They are very sensitive, require a low probe concentration (≤1 mol %), causing negligible perturbation of membrane lipid composition, and can be monitored continuously. Nevertheless, the most frequently used FRET pair (N-NBD-PE and N-Rh-PE) uses headgroup-attached fluorescent probes and thus is sensitive to environmental properties such as ionic strength, hydration, and the presence of divalent cations, quenchers, and chemically active substances (*8*, *9*). Another assay using acyl chain-attached DPH_p-PC (*5*) is devoid of these shortcomings, but uses a relatively high probe concentration (5 mol %) and is rather photosensitive. We introduce here a new lipid mixing assay based on energy transfer between fluorescent probes BODIPY500 and BODIPY530 attached to the acyl chains of phospholipids (PC and PE). For several reasons, BODIPY fluorophores are very attractive compared to other fluorophores used to label lipids (particularly NBD). First, the hydrophobic character of BODIPY groups makes them stay in a deeply buried position within the bilayer (*10*), unlike the NBD group that loops back to the headgroup region (*11*). Second, the high fluorescence quantum yield provides a

† Supported by U.S. Public Health Service Grant GM 32707 to B.R.L.

* To whom requests for reprints should be addressed. E-mail: uncbrl@med.unc.edu.

‡ Current address: The Liposome Co., One Research Way, Princeton, NJ 08540.

§ These authors contributed equally to this work.

[1] Abbreviations: SUVs, small unilamellar vesicles; BODIPY530/550 C_{12}-HPE, 2-(4,4-difluoro-5,7-diphenyl-4-bora-3a,4a-diaza-s-indacene-3-dodecanoyl)-1-hexadecanoyl-*sn*-glycero-3-phosphoethanolamine; β-BODIPY500/510 C_{12}-HPC, 2-(4,4-difluoro-5,7-diphenyl-4-bora-3a,4a-diaza-s-indacene-3-dodecanoyl)-1-hexadecanoyl-*sn*-glycero-3-phosphocholine; Rh-PE, *N*-(lissamine rhodamine B sulfonyl)dioleoylphosphatidylethanolamine; NBD-PE, *N*-(7-nitrobenz-2-oxa-1,3-diazol-4-yl)dioleoylphosphatidylethanolamine; DPH_pPC, 1-palmitoyl-2-[2-4-(phenyl-*trans*-1,3,5-hexatrienyl)phenylethyloxylcarbonyl]-3-*sn*-phosphatidylcholine; FRET, fluorescence resonance energy transfer; DOPC, 1,2-dioleoyl-3-*sn*-phosphatidylcholine; DOPE, 1,2-dioleoyl-3-*sn*-phosphatidylethanolamine; SOPC, 1-stearoyl-2-oleoyl-3-*sn*-phosphatidylcholine; DPPC, 1,2-dipalmitoyl-3-*sn*-phosphatidylcholine; Ch, cholesterol; TES, *N*-[tris(hydroxymethyl)methyl]-2-2-aminoethanesulfonic acid; PEG, poly(ethylene glycol); $C_{12}E_8$, dodecyloctaethylene glycol monoether; DiI, 1,1-dihexadecyl-3,3,3′,3′-tetramethylindocarbocyanine perchlorate.

10.1021/bi010570r CCC: $20.00
Published on Web 06/22/2001

strong fluorescence signal. This, along with the high FRET efficiency of this particular pair (*12*), allows one to use low probe concentrations (≤0.5 mol %) to monitor lipid mixing. Finally, BODIPY analogues are more photostable than NBD and DPH, which is important for long-term kinetic measurements. The results presented here indicate that BODIPY-labeled lipids can be used to obtain reliable and accurate quantitative measurements of lipid mixing without significantly perturbing the process they are intended to follow. By contrast, our results also show that the widely used N-NBD-PE and N-Rh-PE pair reports a reduced rate of lipid movement compared to the rate of either of the chain-labeled probes we examined.

MATERIALS AND METHODS

2-(4,4-Difluoro-5,7-diphenyl-4-bora-3a,4a-diaza-s-indacene-3-dodecanoyl)-1-hexadecanoyl-*sn*-glycero-3-phosphoethanolamine (*β*-BODIPY530/550 C_{12}-HPE), 2-(4,4-difluoro-5,7-diphenyl-4-bora-3a,4a-diaza-s-indacene-3-dodecanoyl)-1-hexadecanoyl-*sn*-glycero-3-phosphocholine (*β*-BODIPY500/510 C_{12}-HPC), *N*-(lissamine rhodamine B sulfonyl)dioleoylphosphatidylethanolamine (Rh-PE), *N*-(7-nitrobenz-2-oxa-1,3-diazol-4-yl)dioleoylphosphatidylethanolamine (NBD-PE), and 1-palmitoyl-2-[2-4-(phenyl-*trans*-1,3,5-hexatrienyl)phenylethyloxylcarbonyl]-3-*sn*-phosphatidylcholine (DPH_pPC) were purchased from Molecular Probes (Eugene, OR). Chloroform stock solutions of 1,2-dioleoyl-3-*sn*-phosphatidylcholine (DOPC), 1,2-dioleoyl-3-*sn*-phosphatidylethanolamine (DOPE), and 1-stearoyl-2-oleoyl-3-*sn*-phosphatidylcholine (SOPC) were purchased from Avanti Polar Lipids, Inc. (Birmingham, AL) and used without further purification. The concentrations of all the stock lipids were determined by phosphate assay (*13*). Cholesterol (Ch) was purchased from Avanti Polar Lipids and was further purified as previously reported by Schwenk et al. (*14*). *N*-[Tris(hydroxymethyl)methyl]-2-aminoethanesulfonic acid (TES) was purchased from Sigma Chemical Co. (St. Louis, MO). Poly(ethylene glycol) with a molecular weight of 7000−9000 (PEG 8000) was purchased from Fisher Scientific (Fairlane, NJ) and further purified as previously reported (*15*). Dodecyloctaethylene glycol monoether ($C_{12}E_8$) was purchased from Calbiochem (La Jolla, CA). All other reagents were of the highest purity grade available.

Vesicle Preparation. Small, unilamellar vesicles were prepared as described previously (*16*). Mixtures of different lipids at appropriate molar ratios with or without the appropriate amount of fluorescent probes in chloroform were dried under a stream of nitrogen. The dried lipids were dissolved in 1 mL of cyclohexane containing 2−3 drops of methanol, frozen on dry ice, and lyophilized under high vacuum overnight. The dried lipids were suspended in an appropriate buffer for 1 h at room temperature. For SUV preparation, the lipid suspension was sonicated for 10 min using a Heat Systems (Plainview, NY) model 350 sonicator equipped with a titanium probe tip 9.5 mm in diameter. Vesicles were fractionated by centrifugation at 70 000 rpm for 25 min at 4 °C using a Beckman TL-100 ultracentrifuge (Palo Alto, CA). All vesicle samples were prepared in buffer containing 100 mM NaCl, 1 mM EDTA, and 10 mM TES (pH 7.4).

Fluorescence. All fluorescence measurements were taken on an SLM 48000 spectrofluorometer (SLM Instruments, Rochester, NY) using a focused 450 W xenon lamp (Ushio Inc.) and equipped with a modified, four-position, multitemperature cuvette holder with constant stirring and operating in T-format. In all experiments, the total lipid concentration was 0.2 mM. All measurements were taken at 23 °C. Probes (B500/530) were excited at 500 nm, and the emission intensity of the donor and acceptor was recorded in channel A at 520 nm and in channel B using a 550 nm cutoff filter (Schott Glass Technologies, Duryea, PA), correspondingly. Lipid mixing values were based on the ratios of donor:acceptor fluorescence as described in the Results. NBD was excited at 460 nm, and emission was monitored in channel A at 530 nm using 8 nm slits. Donor fluorescent intensity was used for lipid mixing calculations using a standard calibration. DPH was excited at 360 nm, and emission intensity was monitored at 430 nm with 8 nm slits.

Lipid Mixing Assays. For measuring the rate of lipid transfer during PEG-induced vesicle fusion, probe-containing vesicles were mixed with probe-free vesicles at a ratio of 1:4. The appropriate amount of PEG solution was added, and the change in fluorescence intensity due to probe dilution was recorded. The percent of lipid mixing was calculated according to eq A4 using standard calibration curves for each probe set obtained from measurements with vesicles containing different probe concentrations. Thus, it was assumed that 100% lipid mixing corresponded to a 5-fold dilution of the probe.

Three different sets of fluorescent probes were used (see structures in Figure 1). For the BODIPY assay, acyl chain-attached lipid probes BODIPY500-PC and BODIPY530-PE were used as the donor and acceptor, respectively, incorporated into probe vesicles at concentrations of 0.5 mol % each.

For the NBD/Rh assay, the FRET pair of probes NBD-PE (donor) and Rh-PE (acceptor) were used as introduced by Struck et al. (*6*). Probe vesicles were prepared with each probe at 1 mol %.

For the DPHpPC assay, an acyl chain-attached lipid probe DPH_pPC was used as developed by Burgess et al. (*5*) with some modifications. In particular, instead of lifetime, we measured fluorescence intensity of the probe that changed during fusion due to dequenching, which then was converted to a lipid mixing value using a standard calibration curve (calibration curve not shown). The calibration curve was fitted by eq A5 (Appendix), and the k (4.03) value was used to calculate the percent lipid mixing. Probe vesicles contained 5 mol % DPH_pPC.

Calculating the Förster Distance. The Förster radius (R_o) was determined from the overlap of donor emission and acceptor excitation spectra according to the Förster equation (*17*):

$$R_o = 0.211[\kappa^2 n^{-4} Q_D J(\lambda)]^{1/6} \quad (1)$$

where κ^2 is a factor describing the relative orientation of the donor and acceptor transition dipoles, n is the refractive index of the hydrophobic core of the lipid bilayer, Q_D is the quantum yield of donor fluorescence in the absence of acceptor, and $J(\lambda)$ is the overlap integral expressing the degree of spectral overlap between the donor emission and

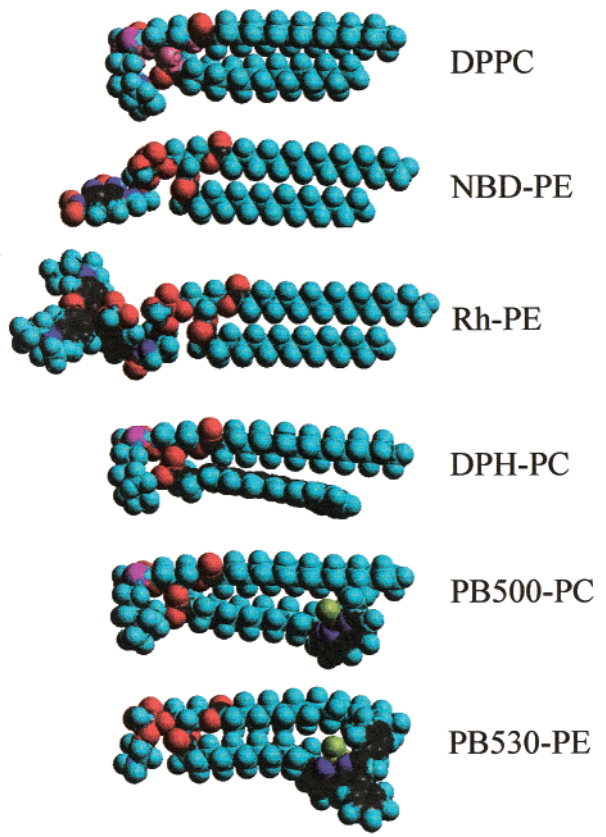

FIGURE 1: Space-filling steric images of 1,2-dipalmitoyl-3-*sn*-phosphatidylcholine (DPPC) and fluorescent probes NBD-PE, Rh-PE, DPH-PC, BODIPY500-PC, and BODIPY530-PE with different atoms represented in light blue (hydrogen), red (oxygen), dark blue (nitrogen), green (boron), purple (phosphorus), and black (carbon).

the acceptor absorption. The overlap integral was normalized by the area of the donor emission spectrum:

$$J(\lambda) = \frac{\int_0^\infty F_D(\lambda)\epsilon(\lambda)\lambda^4\, d\lambda}{\int_0^\infty F_D(\lambda)\, d\lambda} \quad (2)$$

where $\epsilon(\lambda)$ is the extinction coefficient of the acceptor and $F_D(\lambda)$ is the fluorescence of the donor. Equation 1 is valid if the wavelength is expressed in nanometers and the extinction coefficient is in units liters per mole per centimeter (M^{-1} cm^{-1}).

RESULTS

Characterization of a New FRET Lipid Mixing Assay. The emission and excitation spectra of BODIPY500-PC and BODIPY530-PE incorporated into DOPC small unilamellar vesicles are shown in Figure 2A. As one can see, there is a significant overlap between the emission band of BODIPY500-PC and the excitation band of BODIPY530-PE (shaded area in Figure 2A). From this, we can expect to see efficient fluorescence resonance energy transfer (FRET) between this donor/acceptor pair. We used the Förster equation (*17*) (see Materials and Methods for details) to estimate the Förster distance for the BODIPY500-PC and BODIPY530-PE donor/acceptor pair. If one takes the orientation parameter κ^2 to be $^2/_3$ (randomized orientations), the quantum yield of the donor to be 0.95 (*12*), and the

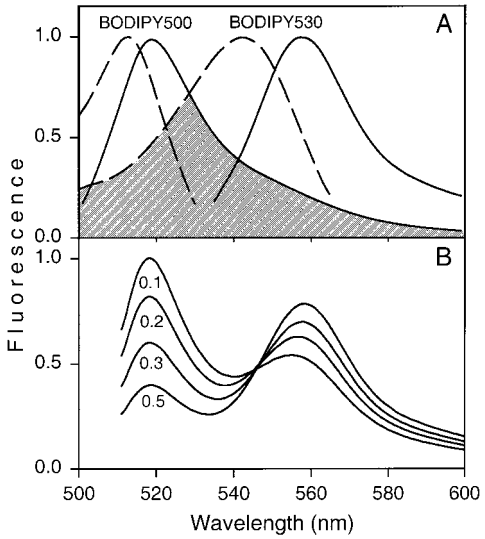

FIGURE 2: (A) Excitation (− − −) and emission (—) spectra of BODIPY500-PC and BODIPY530-PE incorporated into DOPC SUVs at a concentration of 0.1 mol % in units relative to the fluorescence at each peak. The overlap of emission spectra of BODIPY500-PC (donor) and excitation spectra of BODIPY530-PE (acceptor) is shown by the shaded area. (B) Emission spectra of the BODIPY500-PC/BODIPY530-PE mixture in DOPC vesicles at different surface concentrations (mole percent) of each probe as indicated in the figure.

extinction coefficient of the acceptor to be 66 000 M^{-1} cm^{-1} at the absorption maximum of 540 nm (*18*), we obtain an R_o value of ~60 Å.

When the acceptor BODIPY530 is excited at 500 nm [near the excitation maximum of BODIPY500 (512 nm)], the emission spectra of these two probes are reasonably well separated (Figure 2A). The conventional equation for the efficiency of energy transfer (*19*) is

$$E = 1 - F_{DA}/F_D \quad (3)$$

where F_{DA} and F_D are integrated fluorescence intensities of the donor in the presence and absence of the acceptor, respectively. Here it is important that any contribution of the acceptor be removed from the F_{DA} value. Our assay measures F_{don} at 520 nm, where the entire signal comes from BODIPY500. We measure F_{acc} (from the donor in the presence of the acceptor) with a filter that collects intensity mainly above 560 nm. This includes some contribution from donor fluorescence. Thus, our F_{acc}/F_{don} is related to but not equal to E in eq 3. The advantage of this method is that both measurements can be made simultaneously on a T-system fluorometer to yield a quantity unrelated to the concentration of membranes in a sample but still related to the efficiency of energy transfer and thus to the concentration of probes in the membranes. The small contribution of acceptor fluorescence to F_{acc} does not affect our lipid mixing assay, because we used a calibration curve that includes this contribution (see below).

Emission spectra of the BODIPY500-PC/BODIPY530-PE mixtures in DOPC vesicles at different surface concentrations of the probes are shown in Figure 2B and indicate both efficient FRET and high sensitivity of the FRET to the surface probe concentration range that was examined. It is worth noting that donor and acceptor emission peaks are well separated. This provides an opportunity to record not only

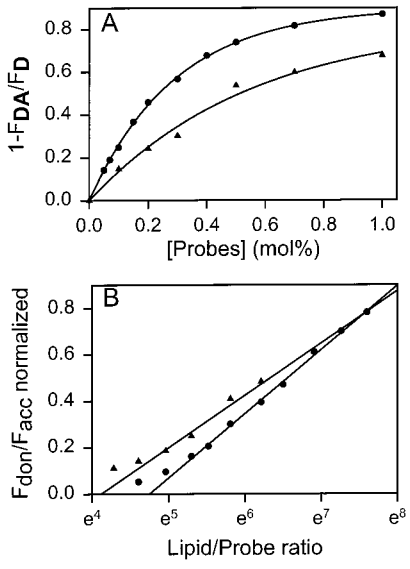

FIGURE 3: Calibration of BODIPY500-PC/BODIPY530-PE (●) and NBD/Rh-PE (▲) fluorescence in DOPC vesicles. Vesicles were prepared with different concentrations of the probes at a 1:1 ratio to yield spectra as shown in Figure 2B. (A) Conventional calibration curves plotted as the FRET efficiency vs probe surface concentration. (B) Donor to acceptor fluorescence ratio as a function of the lipid:probe ratio. The data are well fitted by a single-exponential equation (see eq A5) in the range of 0.05−0.5 mol %, as shown.

the decrease in donor fluorescence but also the increase in acceptor fluorescence as the probe surface concentration increases.

The dependence of FRET efficiency on the surface density of the donor and acceptor is shown in Figure 3. The conventional way of representing FRET efficiency versus probe surface concentration (Figure 3A) suggests fairly efficient energy transfer for the BODIPY pair (●), as the donor fluorescence is quenched significantly at a low probe concentration (0.5 mol %). The calibration curve for the Rh/NBD pair (▲) showed less energy transfer, which could be a result of a shorter R_o or the different probe localization. BODIPY-labeled probes are localized closer to the middle of the bilayer, while Rh and NBD are in the lipid headgroup and thus at the membrane surface. This makes it difficult to calculate the Förster distance for the BODIPY pair from Figure 3A because we do not know how energy transfer between opposite monolayers contributes to the total energy transfer.

We have also plotted the calibration curve in another way, using the ratio of donor to acceptor fluorescence instead of just donor fluorescence in the presence and absence of the acceptor (Figure 3B). As one can see, in this presentation, the data are fitted well with a single exponential in the range of probe surface concentration from 0.05 to 0.5 mol % (see eq A5 in the Appendix). To make a quantitative estimation of the extent of lipid mixing, one should use calibration curves for the lipid:probe ratio as a function of F_{don}/F_{acc} as shown in Figure 3B, making it easy to estimate the extent of lipid mixing from eq A6. In this interpretation, we need only the exponential parameter k from the calibration curve. From our results for DOPC vesicles (Figure 3B), k was 3.7, and it did not vary significantly around this value for vesicles of different compositions (within 10%) (see Table 1). The calibration parameters were also insensitive to changes in membrane hydration, since adding PEG up to 10 wt % did not affect the calibration curve.

Table 1: Parameters Describing the Calibration of the BODIPY Probe Pair in Different Lipid Compositions

	SOPC	DOPC	PC/PE	PC/PE/SM/Ch
A_o	119	112	115	114
k	3.80	3.7	3.49	3.65

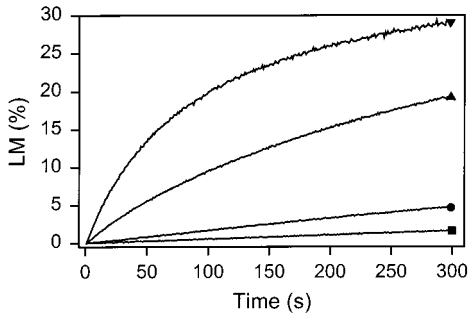

FIGURE 4: PEG-induced fusion of SUVs composed of PC, PE, and Ch [2:1:1 (▼)], PC and PE [3:1 (▲)], DOPC (●), and SOPC (■). Representative kinetics of lipid mixing at 5 wt % PEG are shown. PEG was added to the mixture (1:4 ratio) of probe-containing vesicles (0.5 mol % BODIPY500/530) and probe-free vesicles. The total lipid concentration was 0.2 mM.

The calibration data for the Rh/NBD pair are shown in Figure 3B for comparison. This curve has a shape similar to that for the BODIPY pair, but the slope (or sensitivity to the probe concentration change or the extent of lipid mixing) is smaller.

Expressing the calibration curve as shown in Figure 3B not only allows for a single calibration constant but also produces two additional benefits. First, the assay sensitivity is increased because the donor fluorescence increases (loss of quenching) while the acceptor fluorescence decreases (loss of FRET) with the decrease in probe surface concentration during fusion. Second, the use of this ratio makes the signal intensive; i.e., it does not depend on the total amount of probe in the cuvette. To further ensure a calibration curve in terms of absolute values independent of instrument setup, we normalized the FRET ratio by dividing it by the ratio obtained after adding detergent to the sample. Third, dividing two fluorescent signals reduces signal noise due to scattering from large particles in an inhomogeneous sample.

Application of the New FRET Assay to Measurements of Lipid Mixing Rates. Using the calibration parameter derived in Figure 3, we were able to record the kinetics of PEG-induced lipid mixing between SUVs (Figure 4). To obtain initial rates of lipid mixing from such data, we fitted time courses such as those in Figure 4 with a straight line (slow lipid mixing), or single or double exponentials (intermediate and fast rates of lipid mixing). The initial rates of lipid mixing were then calculated using the best-fit parameters. The rates of lipid mixing between SOPC (■), DOPC (●), DOPC/DOPE [3:1 (▲)], and DOPC/DOPE/Ch [2:1:1 (▼)] vesicles were in the following order: DOPC/DOPE/Ch > DOPC/DOPE > DOPC > SOPC. We have recently reported that the abilities of these vesicles to fuse, as judged by the extent of contents mixing, were also in this order (*20*). Figure 5A shows the initial rate of lipid mixing as a function of added PEG concentration for these four vesicle systems. Remarkably, we found a significant rate of lipid mixing in DOPC/

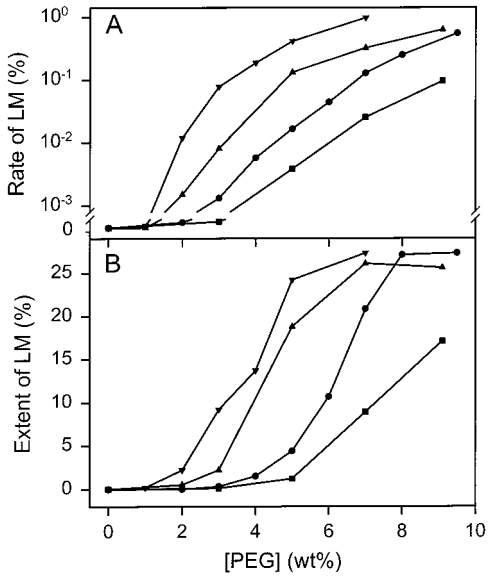

FIGURE 5: PEG-induced fusion of SUVs made of PC, PE, and CH [2:1:1 (▼)], PC and PE [3:1 (▲)], DOPC (●), and SOPC (■) as a function of PEG concentration. (A) Initial rates of lipid mixing. (B) Extent of lipid mixing measured after incubation for 5 min. Errors in the rates or extents of lipid mixing obtained from repeats with a single vesicle preparation were usually 2−4%. Variations between preparations were somewhat larger (see Figure 6).

DOPE/CH and DOPC/DOPE vesicles at PEG concentrations just sufficient to induce aggregation (2−3 wt %) even though DOPC/DOPE vesicles did not show significant contents mixing until 3−5 wt % PEG (*20*).

Due to the difficulty of measuring the fluorescence lifetime of DPHpPC, we have in the past made only one major study of the kinetics of PEG-mediated lipid mixing (*21*, *22*), being content other times with monitoring the extent of lipid mixing after some fixed time. To compare this approach to the kinetic approach, we show in Figure 5B the PEG profile for the extent of lipid mixing in terms of values after incubation for 5 min. It is clear from comparing panels A and B of Figure 5 that using the BODIPY probe pair to monitor the kinetics of lipid mixing provides a much more sensitive view of the fusion process than we can obtain using the single-point assay that we have often used with the DPHpPC probe, especially at low PEG concentrations. For example, lipid mixing between SOPC vesicles (■) was barely perceptible at 5 wt % PEG even up to 300 s (Figure 4), yet the rate of lipid mixing between these vesicles could be conveniently compared to that for more fusogenic vesicles (Figure 5). The BODIPY500-PC/BODIPY530-PE pair, along with the composition-independent calibration curve shown in Figure 3B, makes such initial rate measurements routinely possible. It is next appropriate to ask whether this probe pair can report accurately the movement of normal lipids or whether the presence of bulky fluorophores causes the behavior of the probes to be significantly different from that of normal lipids.

Comparison with Two Other Lipid Mixing Probe Systems. Since it is impossible to compare the behavior of this new lipid mixing probe system with the behavior of unlabeled lipids, we set out to compare it with the behavior of the most widely used lipid-mixing probes that are actually phospholipid molecules, Rh-PE and NBD-PE. We also sought to compare the behavior with that of the probe that we have used for some time to monitor lipid mixing, DPHpPC, since

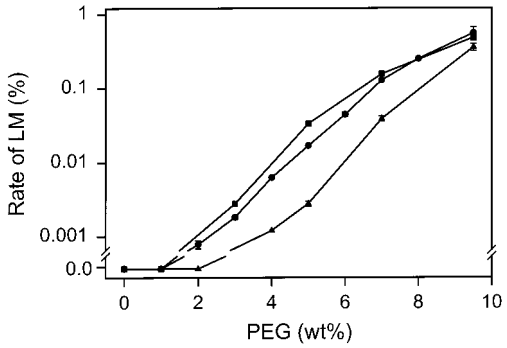

FIGURE 6: Initial rate of lipid mixing of DOPC vesicles shown as a function of PEG concentration as measured by different assays: BODIPY500/530 assay (●), DPHpPC assay (■), and NBD-PE/Rh-PE assay (▲). In general, single vesicle preparations were used for each rate determination, with repeats within that experiment. Variations within a preparation were usually only 2−4%. For selected points, rates were averaged from data from three separate vesicle preparations. Error bars associated with these points (∼10%) represent the standard error of mean.

this molecule is remarkably similar in shape (see Figure 1) and packing properties (*23*) to unlabeled phosphatidylcholine. To make a careful, quantitative comparison, we had to calibrate both these probe systems in the same vesicles used for the BODIPY probe pair. The Rh/NBD calibration curve was well fitted by eq A5 (in the Appendix). The fitting parameter k (4.44) was used for calculation of percent lipid mixing.

Like the BODIPY assay introduced here, the Rh/NBD assay is also based on energy transfer between probes, but unlike the BODIPY assay, the Rh and NBD probes are attached to lipid headgroups of NBD-PE and Rh-PE (Figure 1). The DPHpPC assay is based on an increase in probe fluorescence lifetime during fusion, since DPH undergoes a dimer-dependent excited-state rearrangement that leads to more rapid excited-state decay (*24*). Like the BODIPY probes, the DPH moiety in DPHpPC is attached to an acyl chain (Figure 1). Figure 6 shows the dependence of the initial rate of lipid mixing on PEG concentration as reported by these three different assays. Surprisingly, not all of these results were consistent. While the BODIPY and DPH probes gave very similar results (BODIPY rates only ∼21%/s slower than DPHpPC rates across the PEG profile), the rates obtained with the NBD-PE/Rh-PE pair were roughly 6-fold slower at low PEG concentrations than those obtained with the two other probes. As a result, the thresholds of lipid exchange also differed remarkably, being 2 wt % PEG for DPHpPC or the BODIPY pair and 4 wt % PEG for the NBD-Rh pair.

DISCUSSION

The ideal probe for use in lipid mixing assays should (1) provide a strong, stable fluorescent signal in the visible range, (2) not be affected by changes in the water environment, (3) mimic the shape and behavior of the membrane lipids so as not to distort bilayer structure, (4) provide a signal sensitive to its surface concentration that behaves as an intensive quantity, and (5) not perturb the process it is used to measure. The BODIPY assay presented here meets all of these requirements. The BODIPY fluorophore is known to be photostable and intensely fluorescent with an extremely

high quantum yield (~0.95) when located in the hydrophobic core of a bilayer (*12*). It has the largest excitation and emission wavelengths among currently available phospholipid-labeled probes, which should minimize light scattering in inhomogeneous samples. The BODIPY moieties are fairly hydrophobic groups located at the end of acyl chains (Figure 1), which means they should stay buried inside the membrane, inaccessible to hydrophilic perturbants in the aqueous medium. Thus, the calibration parameters for the BODIPY pair did not change with lipid composition (Table 1) or in the presence of PEG (up to 10%). The chain location of the fluorescent moieties of the BODIPY probes means that the perturbing influence of the fluorophore will be felt in the center of the bilayer, and this should be easily accommodated at a low probe concentration by the chain disorder in this region. The high FRET efficiency (see Figures 2 and 3) and high quantum yield of BODIPY-labeled lipids make the use of low probe concentrations ($\leq$0.5 mol %) feasible. Nonetheless, the best probe in terms of mimicking a lipid should be DPHpPC, whose DPH group looks like the continuation of a normal acyl chain (Figure 1). Unfortunately, DPHpPC must be used at a fairly high concentration to make its fluorescence lifetime sensitive to its membrane concentration.

For any assay of lipid mixing, it is important that the probe that is used not be transferred spontaneously between vesicles. This can be checked simply by incubating the probe and empty vesicles in the absence of stimulus (PEG). In our experiments, the extent of this type of spontaneous probe transfer was estimated to be below 10^{-3} %/s. Upon aggregation, the extent of probe transfer should be much higher and can result from fusion as well as from an increased level of transfer though the thin water layer between juxtaposed bilayers in aggregated vesicles. We can estimate the rate of intervesicle transfer between closely juxtaposed bilayers from our measurements on SOPC SUVs at 3 wt % PEG. Aggregation definitely occurs under these conditions as does fusion of more fusogenic vesicles. The rate of BODIPY-labeled lipid transfer between SOPC vesicles in the presence of 3 wt % PEG was less than 0.001%/s. This is much slower than transfer seen during fusion of DOPC/DOPE/Ch vesicles at the same PEG concentration (1%/s). If it is assumed that the spontaneous intervesicle transfer rate does not depend on vesicle composition, then the contribution of spontaneous probe transfer to lipid mixing between fusogenic vesicles (such as DOPC/DOPE/Ch) is negligible.

While the occurrence of intervesicle lipid transfer during the fusion process should be easily followed by a variety of probes, a lipid probe used for monitoring the kinetics of lipid mixing should move between vesicles in a manner that mimics the behavior of unlabeled lipids. Since there is no way to monitor intervesicle movement of an unlabeled probe, we have compared our new BODIPY assay with the popular assay based on FRET of the NBD-PE/Rh-PE pair and with our assay based on excited-state dimerization of DPHpPC. We reasoned that if all three assays gave comparable results, it would verify all three. The fact that the BODIPY500/BODIPY530 assay and the DPHpPC fluorescence dequenching assays were consistent with each other but both disagreed with the NBD-PE/Rh-PE FRET assay was quite unexpected and caused us to ask the following: what is so different about these probes that they should produce inconsistent results? The answer to this question lies, we believe, in the structure of these molecules (Figure 1). What we can see clearly is that DPHpPC is almost indistinguishable from an unlabeled DPPC molecule. BODIPY500-PC and especially BODIPY530-PE are slightly cone shaped and probably would show a negative spontaneous curvature. But in the case of NBD-PE and especially Rh-PE, bulky fluorescent groups attached to the headgroups should give these two lipids distinctly positive intrinsic curvatures. This is confirmed in the case of Rh-PE (*25*). We know that positively curved lyso-PC inhibits fusion even at a concentration as low as 1 mol % (*26*, *27*). So it would be reasonable to suggest that these lipid probes would also affect fusion. It is also possible that probe diffusion through the first fusion intermediate could be suppressed even without affecting fusion rate. Specifically, it is possible that the stalk intermediate, with a very high negative curvature of the contacting leaflets (*28*), would provide a substantial free energy barrier for movement of probes with positive intrinsic curvatures, especially since they would be moving from vesicle outer monolayers having a slight positive curvature. This could offer a substantial additional free energy barrier to the diffusion of NBD-PE and especially Rh-PE between fusing membranes. This means that the stalk structure should inhibit movement of probes having large fluorescent moieties attached to their polar headgroups but would not inhibit and perhaps even would favor movement of probes with a negative intrinsic curvature. The BODIPY probes introduced in this paper both should have negative intrinsic curvatures and thus partition favorably into the connecting cis leaflets of the stalk structure. We tried to test whether inhibition of lipid mixing by Rh/NBD-PE was linked to inhibition of fusion using the Tb/DPA contents mixing assay in the presence of the Rh/NBD-PE and BODIPY pairs. Unfortunately, we found that Tb/DPA fluorescence was significantly quenched in the presence of Rh/NBD-PE. We will pursue this issue soon with other lipid molecules having molecular shapes similar to the those of the Rh-PE and BODIPY probes.

On the basis of the arguments and observation presented here, the ability of a lipid probe to report lipid mixing associated with fusion of pure lipid bilayers is expected to depend on the intrinsic shape of the lipid molecule. A recent paper (*29*) provides a quantitative comparison of lipid mixing associated with protein-mediated biomembrane fusion as detected by different probes. This paper examined the chronological relation between the establishment of lipid continuity (detected using self-quenching of different lipid dyes) and fusion pore formation (detected by conductivity measurements) during hemagglutinin-induced fusion of HA-expressing cells to a planar lipid bilayer. According to this report, fusion pores always formed before detectable amounts of Rh-PE moved from the bilayer to a cell. However, the relationship of fusion pore formation and lipid dye movement was reversed when DiI (1,1-dihexadecyl-3,3,3′,3′-tetramethylindocarbocyanine perchlorate) was used as the lipid probe. The authors explained the more rapid movement of DiI than of Rh-PE in terms of the fact that DiI readily flip-flops between monolayers of a bilayer membrane whereas Rh-PE does not (*30*). On the basis of our results, there is another possible explanation, namely, that the bulky labeled headgroup of Rh-PE (see Figure 1) hampers movement of probes through the stalk between fusing membranes, and thus reduces the reported rate of lipid mixing. The restricted

transfer of the DiI probe between HA-induced fusing cells has been widely reported (*31*−*33*) and suggested to be due to HA proteins forming a ring around the initial fusion intermediate and thus restricting lipid redistribution between two hemifused membranes. Our results do not challenge this proposal but do demonstrate that the rate of lipid probe movement through the initial fusion intermediate can reflect the physical properties of both the probe and the intermediate as well as the presence of the fusion protein machinery.

APPENDIX

Calculation of the Extent of Lipid Mixing. Let us assume that, during vesicle fusion, each probe vesicle fuses with gradually increasing numbers of probe-free vesicles until, on average, it fuses with n vesicles, where n is the ratio of probe-free to probe-containing vesicles in a sample. This process takes place in a vesicle aggregate (*34*) and clearly involves a distribution of possible pairings of probe-containing and probe-free vesicles to form aggregates that are available to form final fusion products (*35*). Normally, one makes the assumption that the ratio of probe-free to probe-containing vesicles in the dominant aggregate is the same as the ratio in the overall sample, i.e., n. As fusion proceeds, we assume that some number of probe-free vesicles, $x(t)$, have fused with each probe-containing vesicle in an aggregate by time t. Then the fraction lipid mixing (LM) is

$$\mathrm{LM} = x(t)/n \tag{A1}$$

For all three assays, we measure a change in fluorescence due to dilution of probe molecules during fusion. On the basis of this model, the lipid:probe ratio in an average fusing probe-containing vesicle within an aggregate is increased by the addition of lipids from $x(t)$ fusing probe-free vesicles. Thus, the lipid:probe ratio becomes

$$L/P(t) = (L/P)_0[1 + x(t)] \tag{A2}$$

where $x(t)$ is presumed to increase from 0 to n as fusion proceeds. Here $(L/P)_0$ is the original lipid:probe ratio in a probe-containing vesicle before fusion. Taking eqs A1 and A2 together, we obtain

$$L/P(t) = (L/P)_0[1 + n\mathrm{LM}(t)] \tag{A3}$$

or

$$\mathrm{LM}(t) = \frac{[L/P(t)]/(L/P)_0 - 1}{n} \tag{A4}$$

As we found from the calibration curve (Figure 3B), L/P as a function of the fluorescence of the donor:acceptor ratio (for the BODIPY500/530 pair) is fit well by a single exponential in the range of probe concentrations of 0.05−0.5 mol

$$L/P = A \exp[k(F_{\mathrm{don}}/F_{\mathrm{acc}})] \tag{A5}$$

where A is a scaling constant, F_{don} and F_{acc} are the fluorescence intensities of the donor and acceptor, respectively, and k is an exponential constant.

Substituting eq A5 into eq A4, we have

$$\mathrm{LM}(t) = \frac{1}{n}\{e^{k[(F_{\mathrm{don}}/F_{\mathrm{acc}}) - (F_{\mathrm{don}}/F_{\mathrm{acc}})_0]} - 1\} \tag{A6}$$

Thus, for quantitative determination of LM(t), we need only the exponential parameter k obtained from the calibration curve. To obtain the initial rate of lipid mixing from measured time-dependent fluorescence traces, we simply differentiate eq A6 with respect to time, with the only time-dependent quantity being the measured $F_{\mathrm{don}}/F_{\mathrm{acc}}$:

$$(\mathrm{dLM}/\mathrm{d}t)_{t=0} = k/n[\mathrm{d}(F_{\mathrm{don}}/F_{\mathrm{acc}})/\mathrm{d}t]_{t=0}$$

REFERENCES

1. Owen, C. S. (1980) *J. Membr. Biol. 54*, 13−20.
2. Pal, R., Barenholz, Y., and Wagner, R. R. (1988) *Biochemistry 27*, 30−6.
3. Nichols, J. W. (1987) *J. Biol. Chem. 262*, 14172−7.
4. Bisgaier, C. L., Minton, L. L., Essenburg, A. D., White, A., and Homan, R. (1993) *J. Lipid Res. 34*, 1625−34.
5. Burgess, S. W., and Lentz, B. R. (1993) *Methods Enzymol. 220*, 42−50.
6. Struck, D. K., Hoekstra, D., and Pagano, R. E. (1981) *Biochemistry 20*, 4093−9.
7. Mattjus, P., Molotkovsky, J. G., Smaby, J. M., and Brown, R. E. (1999) *Anal. Biochem. 268*, 297−304.
8. Hong, K., Baldwin, P. A., Allen, T. M., and Papahadjopoulos, D. (1988) *Biochemistry 27*, 3947−55.
9. Stubbs, C. D., Williams, B. W., Boni, L. T., Hoek, J. B., Taraschi, T. F., and Rubin, E. (1989) *Biochim. Biophys. Acta 986*, 89−96.
10. Kaiser, R. D., and London, E. (1998) *Biochim. Biophys. Acta 1375*, 13−22.
11. Chattopadhyay, A., and London, E. (1987) *Biochemistry 26*, 39−45.
12. Johnson, I. D., Kang, H. C., and Haugland, R. P. (1991) *Anal. Biochem. 198*, 228−37.
13. Chen, P. S., Jr., Toribara, T. Y., and Warner, H. (1956) *Anal. Chem. 28*, 1756−8.
14. Schwenk, E., and Werthessen, N. T. (1952) *Arch. Biochem. Biophys. 40*, 334−41.
15. Lentz, B. R., McIntyre, G. F., Parks, D. J., Yates, J. C., and Massenburg, D. (1992) *Biochemistry 31*, 2643−53.
16. Lentz, B. R., Carpenter, T. J., and Alford, D. R. (1987) *Biochemistry 26*, 5389−97.
17. Lakowicz, J. R. (1999) *Principles of fluorescence spectroscopy*, 2nd ed., Kluwer Academic/Plenum Publishers, New York.
18. Haugland, R. P. (1998) *Handbook of fluorescent probes*, 6th ed., Molecular Probes, Eugene, OR.
19. Fung, B. K., and Stryer, L. (1978) *Biochemistry 17*, 5241−8.
20. Haque, M. E., McIntosh, T. J., and Lentz, B. R. (2001) *Biochemistry 40*, 4340−8.
21. Lee, J., and Lentz, B. R. (1997) *Biochemistry 36*, 6251−9.
22. Lee, J., and Lentz, B. R. (1998) *Proc. Natl. Acad. Sci. U.S.A. 95*, 9274−9.
23. Parente, R. A., and Lentz, B. R. (1985) *Biochemistry 24*, 6178−85.
24. Lentz, B. R., and Burgess, S. W. (1989) *Biophys. J. 56*, 723−33.
25. Razinkov, V. I., Melikyan, G. B., Epand, R. M., Epand, R. F., and Cohen, F. S. (1998) *J. Gen. Physiol. 112*, 409−22.
26. Wu, H., Zheng, L., and Lentz, B. R. (1996) *Biochemistry 35*, 12602−11.
27. Chernomordik, L. V., Vogel, S. S., Sokoloff, A., Onaran, H. O., Leikina, E. A., and Zimmerberg, J. (1993) *FEBS Lett. 318*, 71−6.
28. Chernomordik, L. (1996) *Chem. Phys. Lipids 81*, 203−13.

29. Razinkov, V. I., Melikyan, G. B., and Cohen, F. S. (1999) *Biophys. J. 77*, 3144−51.
30. Melikyan, G. B., Deriy, B. N., Ok, D. C., and Cohen, F. S. (1996) *Biophys. J. 71*, 2680−91.
31. Tse, F. W., Iwata, A., and Almers, W. (1993) *J. Cell Biol. 121*, 543−52.
32. Zimmerberg, J., Blumenthal, R., Sarkar, D. P., Curran, M., and Morris, S. J. (1994) *J. Cell Biol. 127*, 1885−94.
33. Blumenthal, R., Sarkar, D. P., Durell, S., Howard, D. E., and Morris, S. J. (1996) *J. Cell Biol. 135*, 63−71.
34. Talbot, W. A., Zheng, L. X., and Lentz, B. R. (1997) *Biochemistry 36*, 5827−36.
35. Wu, J. R., and Lentz, B. R. (1994) *J. Fluores. 4*, 153−63.

BI010570R